Human Molecular Genetics, 2011 **1–11**
doi:10.1093/hmg/ddr288

Increasing expression and decreasing degradation of SMN ameliorate the spinal muscular atrophy phenotype in mice

Deborah Y. Kwon, William W. Motley, Kenneth H. Fischbeck and Barrington G. Burnett*

Neurogenetics Branch, National Institute of Neurological Disorders and Stroke, NIH, Bethesda, MD, USA

Received February 24, 2011; Revised May 2, 2011; Accepted June 16, 2011

Spinal muscular atrophy (SMA) is a neuromuscular disorder caused by reduced levels of the survival motor neuron (SMN) protein. Here we show that the proteasome inhibitor, bortezomib, increases SMN in cultured cells and in peripheral tissues of SMA model mice. Bortezomib-treated animals had improved motor function, which was associated with reduced spinal cord and muscle pathology and improved neuromuscular junction size, but no change in survival. Combining bortezomib with the histone deacetylase inhibitor trichostatin A (TSA) resulted in a synergistic increase in SMN protein levels in mouse tissue and extended survival of SMA mice more than TSA alone. Our results demonstrate that a combined regimen of drugs that decrease SMN protein degradation and increase SMN gene transcription synergistically increases SMN levels and improves the lifespan of SMA model mice. Moreover, this study indicates that while increasing SMN levels in the central nervous system may help extend survival, peripheral tissues can also be targeted to improve the SMA disease phenotype.

INTRODUCTION

Spinal muscular atrophy (SMA), an autosomal recessive neuromuscular disorder, is one of the leading genetic causes of infant death. SMA results from deletion of the survival of motor neuron-1 (*SMN1*) gene and a consequent deficiency of the SMN protein. Although a second nearly identical gene, SMN2, is retained in SMA patients, the *SMN2* gene primarily produces an alternatively spliced isoform lacking exon 7, which encodes a protein that is largely unstable and rapidly degraded. Multiple copies of *SMN2* in transgenic mice can alleviate severity of the SMA disease phenotype on a *smn* null background, with a gene dosage effect (1). Patients with mild SMA often have multiple *SMN2* copies, and some individuals with four or five *SMN2* genes have been found to be phenotypically normal (2–4). Thus, a promising approach to treating SMA could include increasing levels of functional SMN protein by increasing *SMN2* transcript levels and blocking the degradation of its gene product.

SMN is degraded through the ubiquitin proteasome system (UPS) (5,6). In this system, proteins destined for degradation are targeted by linkage to ubiquitin through the action of various enzymes. Once a chain of four or more ubiquitin moieties is assembled on a protein, it is delivered to the 26S proteasome for proteolysis. Contained within the central core of each 26S proteasome are six active proteolytic sites; two cleave after hydrophobic residues (chymotrypsin-like), two after basic residues (trypsin-like) and two others after acidic residues (caspase-like) (7). Together, these sites catalyze the breakdown of proteins into short oligopeptides. Because the proteolytic sites in the 26S proteasome function by different mechanisms, it has been possible to develop drugs that inhibit one or two active sites in the 20S core without rendering the entire proteasome nonfunctional. The clinically used dipeptide boronic acid, bortezomib, is one such drug, which reversibly inhibits chymotrypsin cleavage in the proteasome without affecting the other active sites. Bortezomib was selected from an *in vitro* screen for its pro-apoptotic and anti-tumor profile and is currently approved for treatment of multiple myeloma (8).

In the present study, we targeted the UPS to block the degradation of the SMN protein. Treatment of cultured cells with proteasome inhibitors MG132 and lactacystin has already been shown to increase SMN protein levels; however, these drugs are not amenable for therapeutic use due to their off-target effects and toxicity (5). In this study,

*To whom correspondence should be addressed at: Neurogenetics Branch, NIH, Building 35, Room 2A1008, Bethesda, MD 20892, USA. Tel: +1 3014359288; Fax: +1 3014803365; Email: burnettb@ninds.nih.gov

we characterized bortezomib's effect on SMN protein levels in SMA patient-derived cell lines and on the SMA phenotype in SMA model mice. We asked whether we could synergistically increase SMN protein levels by combining bortezomib with trichostatin A (TSA), a histone deacetylase (HDAC) inhibitor previously shown to upregulate *SMN* gene transcription (9,10). Our study demonstrates that a two-drug regimen that increases gene transcription and stabilizes protein levels may be a promising therapy for SMA, and that peripheral tissues, such as the muscle, may be targeted to improve the SMA phenotype.

RESULTS

Bortezomib increases SMN in SMA fibroblasts and in peripheral tissues of SMA mice

SMA patient-derived fibroblasts were treated with the commercially available proteasome inhibitor, bortezomib (Velcade®, previously PS-341), to determine whether it increases SMN protein levels. Similar to previously published results using other proteasome inhibitors, SMN levels increased in a dose-dependent manner in the presence of bortezomib (Fig. 1A). This correlated with an accumulation of ubiquitinated SMN, indicating that the increase in SMN protein was due to proteasome inhibition rather than to off-target effects of the drug (Fig. 1B). Given bortezomib's ability to increase SMN and its low toxicity compared with other proteasome inhibitors, we then proceeded to test the drug in SMA model mice.

To study bortezomib's efficacy *in vivo*, we treated SMA pups (SMN2 +/+, SMNΔ7, Smn−/−) by intraperitoneal (i.p.) injections (0.15 mg/kg) starting at P5 and continuing every other day. This was the maximum tolerated dose for mice at this age. SMA pups were treated until P13 and then sacrificed to examine SMN levels in various tissues by western blot. We observed an approximately 2-fold SMN increase in the liver, muscle and kidney of bortezomib-treated mice, while levels of SMN in the spinal cord and brain remained unchanged (Fig. 2). Bortezomib has low central nervous system (CNS) penetrance, and brain and spinal cord tissues from bortezomib-treated animals showed no change in proteasome activity (Supplementary Material, Fig. S1). Since SMN levels in the peripheral nervous system could be increased by bortezomib treatment and affect SMN levels in the anterior horn cells (AHCs) of the spinal cord, we stained lumbar spinal cord sections in vehicle- and bortezomib-treated mice. However, we did not observe a significant difference in SMN levels in the AHC of bortezomib-treated mice compared with those treated with vehicle (Supplementary Material, Fig. S2).

Bortezomib improves motor function of SMA model mice but does not extend lifespan

We then asked whether the increase in SMN protein levels we observed in peripheral tissues is sufficient to ameliorate the SMA phenotype. SMA mice were given bortezomib (0.15 mg/kg) as described above, but with treatment continuing until weaning at P21. Motor function was assessed daily as the average time it took for the mice to right themselves once placed on their backs. The righting times of bortezomib-treated animals were improved starting at P8 (Fig. 3B; $P = 0.01$). However, bortezomib had no overall effect on the survival of these mice, although some decrease in early deaths was observed (Fig. 3A). These results suggest that an increase in SMN protein levels in peripheral tissues may improve motor behavior, but that increased SMN in the CNS may be required for an extension of lifespan.

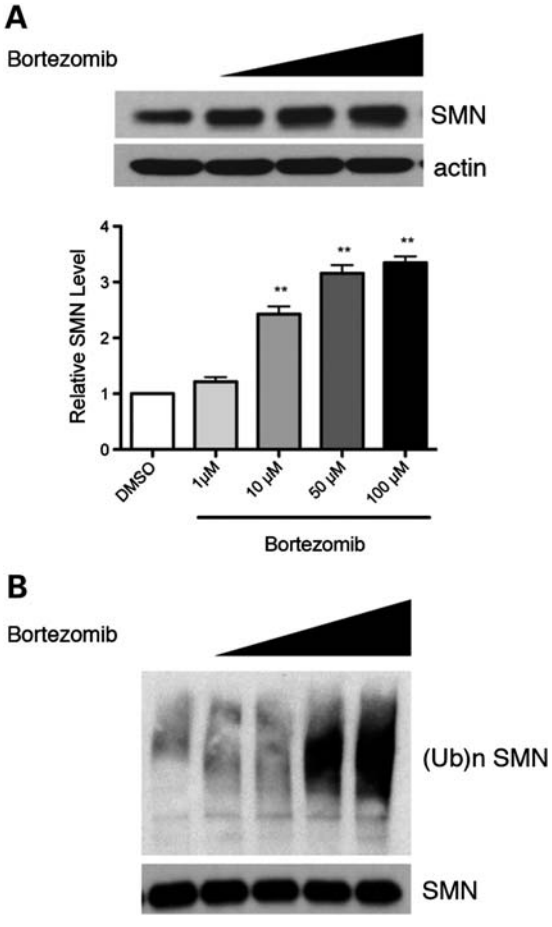

Figure 1. SMN is increased in bortezomib-treated cells. (**A**) SMA patient fibroblasts treated for 16 h with different doses (1, 10, 50 and 100 μM, respectively) of the proteasome inhibitor bortezomib showed dose-dependent increases in SMN protein levels. Quantification is shown in lower panel. (**B**) HEK 293T cells treated with bortezomib have increased SMN ubiquitination in a dose-dependent manner. Values represent mean ± SEM of three independent experiments. $^{**}P < 0.01$.

Bortezomib and TSA synergistically increase SMN protein levels and improve survival and motor function in SMA model mice

Since our data showed that bortezomib treatment blocks SMN degradation in the peripheral tissues of mice, we next asked whether upregulating the *SMN2* gene throughout the mouse might synergize with bortezomib and confer a greater therapeutic effect on the SMA phenotype *in vivo*. To test this hypothesis, we used a combined regimen of bortezomib and TSA, a CNS-penetrant HDAC inhibitor that has been previously shown to increase SMN transcript levels *in vitro* and

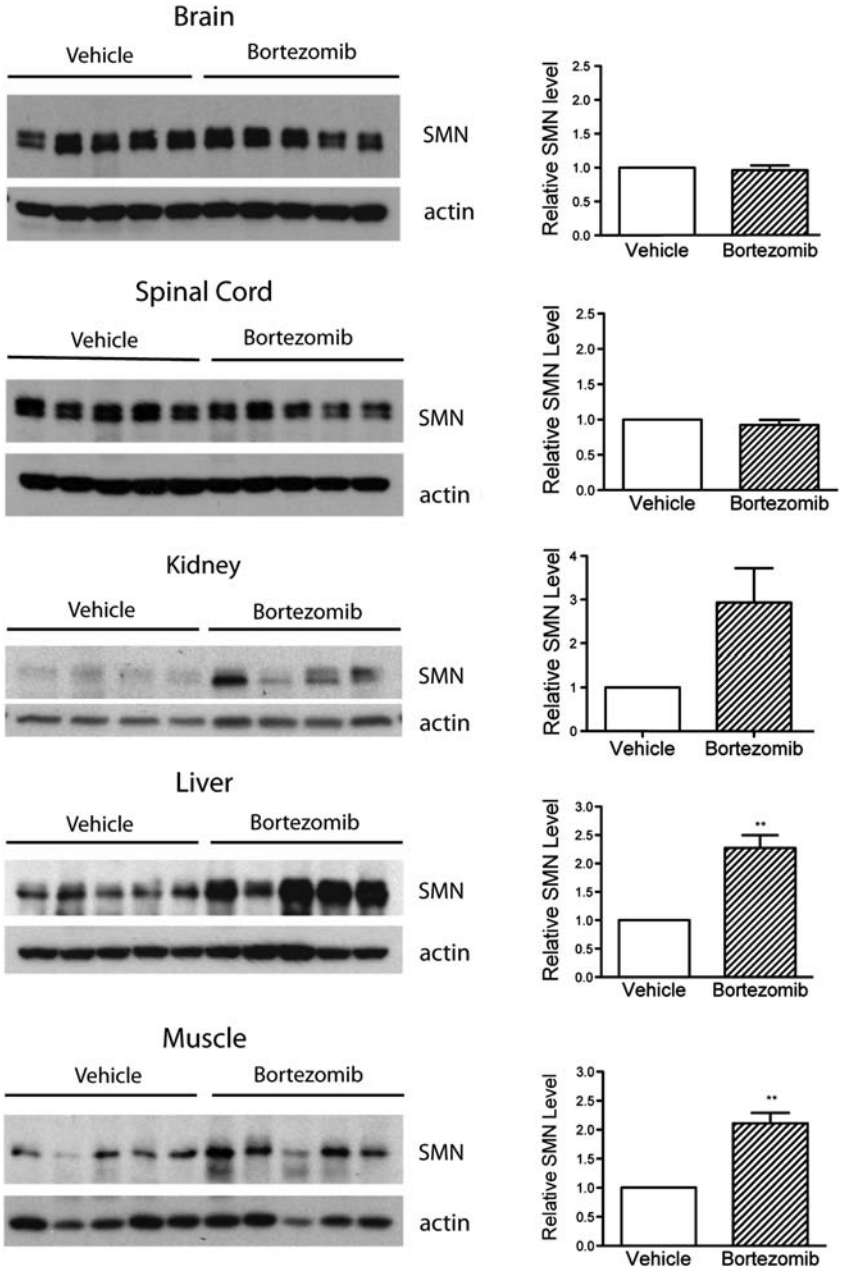

Figure 2. Bortezomib increases SMN protein levels *in vivo*. Mice at P5 were treated with either bortezomib (0.15 mg/kg) or vehicle (water) every other day and sacrificed at P13. The brain, spinal cord, liver, kidney and muscle tissues were removed, and protein lysates were isolated for biochemical analysis. A densitometry analysis was performed on the resulting western blots to ascertain relative SMN protein levels in each tissue. Values represent mean ± SEM. $^{**}P < 0.01$.

in vivo (9). Treatment of SMA patient-derived fibroblasts with either drug alone increased SMN protein levels but giving both drugs together was additive, consistent with the actions of the drugs on distinctive pathways (Supplementary Material, Fig. S3).

We next sought to determine whether delivery of both bortezomib and TSA affects the SMA phenotype in the mice. Since inhibition of the proteasome can last for up to 48 h (data not shown), mice were treated every other day with bortezomib and daily with TSA, starting at P5. In order to mitigate the toxicity we observed administering both drugs together, we reduced the dose of TSA to 4 mg/kg and bortezomib to 0.075 mg/kg. We found that even at this lower dose, SMN protein levels were increased in tissues from TSA-treated mice compared with those treated with vehicle (Supplementary Material, Fig. S4). In all tissues isolated, SMN protein levels were significantly increased in TSA- and bortezomib-treated animals at P13 compared with those treated with vehicle alone (Fig. 4). SMN was increased in peripheral tissues above levels observed with either bortezomib (Fig. 4) or TSA alone (Supplementary Material, Fig. S4) when both drugs were co-administered.

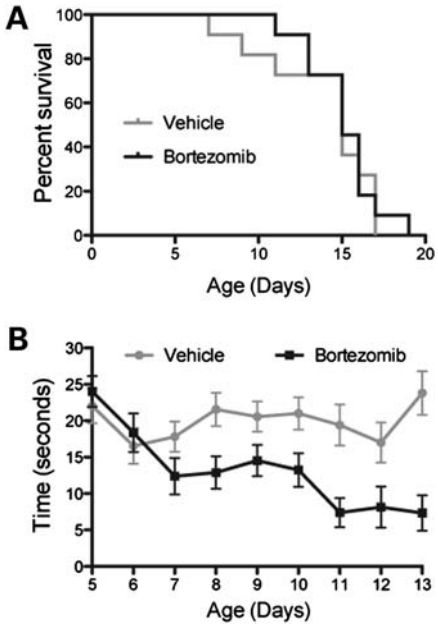

Figure 3. Bortezomib improves motor function; does not affect survival. SMA mice were treated with i.p. injections of bortezomib (0.15 mg/kg) or vehicle (water) every other day starting on P5. (**A**) Survival curves of SMA mice treated with bortezomib or vehicle (log-rank test, $P = 0.76$; $n = 12$ bortezomib; $n = 10$ vehicle). (**B**) Righting time in SMA mice treated with bortezomib ($n = 12$) or vehicle ($n = 10$).

Combining TSA and bortezomib treatment also extended the survival of SMA mice more than TSA alone. Mice treated with 4 mg/kg of TSA lived ~3 days longer than vehicle [dimethyl sulfoxide (DMSO)]-treated mice similar to effects reported with 10 mg/kg of TSA (9); however, average lifespan was increased to 6 days when both TSA and bortezomib were given in combination (Fig. 5A). While we observed a similar improvement in the righting times of TSA only and TSA- and bortezomib-treated mice ($P = 0.37$), we found that animals treated with both drugs gained more weight over the course of treatment on average than those treated with either TSA alone (Fig. 5B; $P < 0.05$) or vehicle (Fig. 5B; $P < 0.001$).

Bortezomib and TSA improve the motor unit pathology in SMA mice

Based on the motor improvement we observed with TSA and bortezomib treatment, we next examined whether there was structural improvement of the motor unit. Cohorts of vehicle-, bortezomib-, TSA- and TSA plus bortezomib-treated mice were sacrificed at P13, and muscle and spinal cord tissues were isolated for histological examination ($n = 3$, each group). Hematoxylin- and eosin-stained cross-sections of tibialis anterior (TA) muscles from P13 SMA mice showed a significant increase in myofiber size with either bortezomib ($P < 0.05$) or TSA treatment alone ($P < 0.01$) compared with vehicle-treated mice (Fig. 6). We did not observe a statistically significant increase in myofiber size with the combination of TSA and bortezomib; however, treatment with both drugs further increased myofiber number over what was observed with bortezomib alone ($P < 0.05$) and TSA alone ($P < 0.01$).

We next analyzed the number of neurons >25 μm in diameter in the anterior horn of the lumbar spinal cord. We found a nearly 2-fold increase in the number of AHC per section in mice treated with bortezomib alone or the combination of bortezomib and TSA (Fig. 7A). TSA treatment alone did not increase AHC numbers, consistent with the previously published data (9). Furthermore, there was no significant difference in AHC numbers between mice treated with bortezomib alone and those treated with TSA and bortezomib, indicating that the observed increase was likely an effect of bortezomib alone. We have previously reported that expression levels of choline acetyltransferase (ChAT), a motor neuron marker, are reduced in SMA mice compared with heterozygous littermates (9). To further validate the increase in AHCs observed in drug-treated mice, we also analyzed ChAT levels in these animals by western blot. ChAT levels were only slightly increased in TSA-treated mice (Supplementary Material, Fig. S4B; $P = 0.066$). However, we observed an approximate 4-fold increase in ChAT protein levels in animals treated with bortezomib alone (Fig. 7B; $P = 0.055$) or with the combination of bortezomib and TSA (Fig. 7B; $P = 0.029$), suggesting that these drugs reduce motor neuron loss in SMA mice.

Given the low availability of bortezomib in the CNS, the increase in AHC number in mice treated with the drug was surprising. Recent studies have identified a role for SMN in the maturation of neuromuscular junctions (NMJs), with poor terminal arborization, denervation, impaired synaptic vesicle release, neuronal antigen accumulation and decreased NMJ size in SMA mice. We therefore examined the effect of bortezomib treatment on the NMJ, comparing NMJs in the TA muscles of affected mice at P13. Alpha-bungarotoxin was used to identify the post-synaptic side of the NMJ, and antibodies to synaptic vesicle protein 2 and neurofilament were used to visualize presynaptic morphology. As previously reported, we found that SMA NMJ post-synaptic terminals were small and simplified compared with those in control littermates (Fig. 8). Quantification of the size indicated that the morphology of SMA NMJs was significantly improved with bortezomib treatment alone. TSA alone also improved the mean surface area of SMA NMJs, and an additive effect was observed when both drugs were delivered together. Qualitative comparison also showed that there were incremental improvements in NMJ maturity as indicated by an increase in invaginations in the post-synaptic staining (Fig. 8, white arrows). We then compared the NMJ morphology from SMA mice treated with TSA and bortezomib and unaffected littermates at P19. The NMJs in TSA- and bortezomib-treated mice continued to mature between P13 and P19, and by P19 appeared similar to control littermates (Supplementary Material, Fig. S5). Our results suggest that the motor improvements we observed in SMA mice treated with bortezomib alone could be due to improvement at the NMJ and that extended survival in TSA- and bortezomib-treated mice may be due to amelioration of motor unit pathology. We note that TSA also increases NMJ size but does not increase AHC number, suggesting that TSA and bortezomib affect the CNS by different mechanisms.

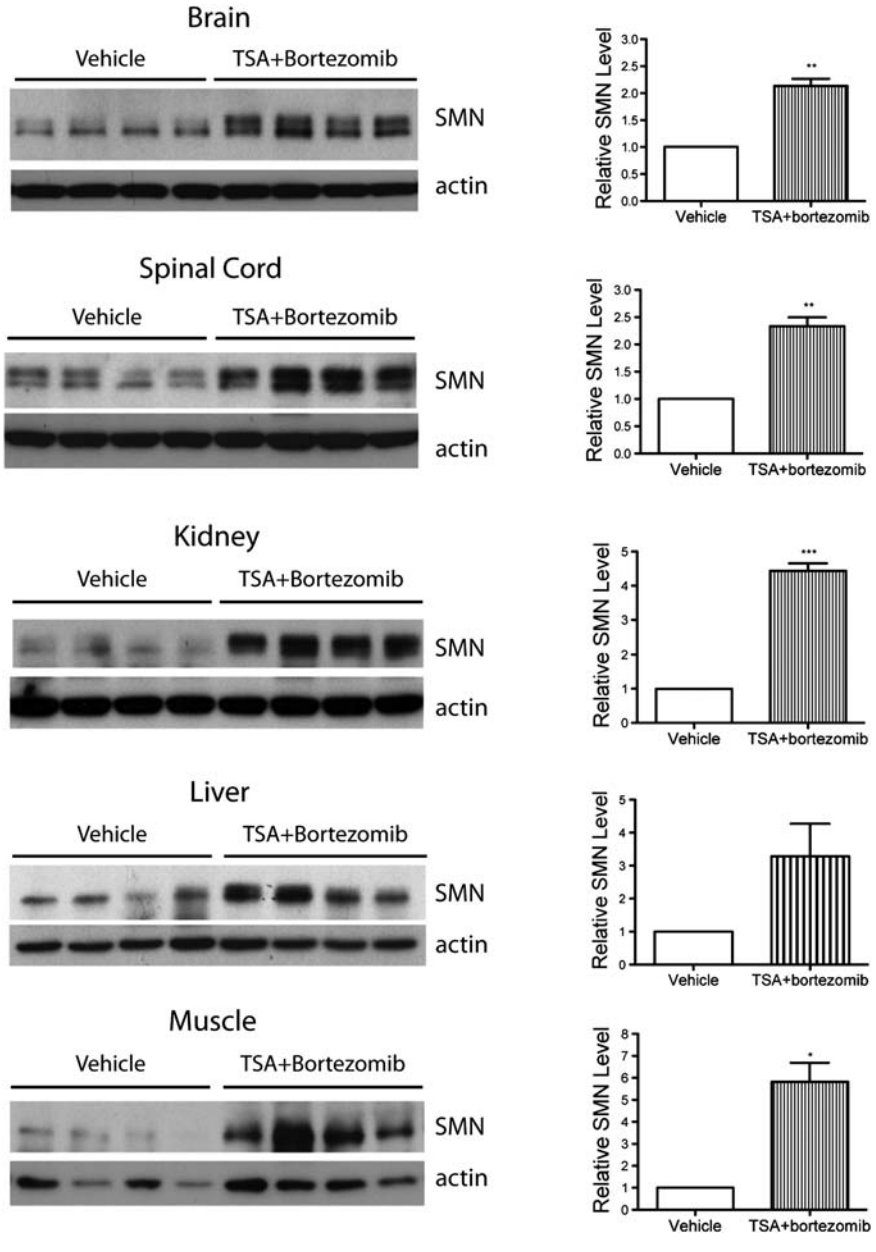

Figure 4. Combining trichostatin A and bortezomib increases SMN *in vivo*. SMA mice aged P5 were treated with TSA (4 mg/kg) and bortezomib (0.075 mg/kg) or with vehicle (DMSO and water). Mice were sacrificed for biochemical analysis at P13. The brain, spinal cord, liver, kidney and muscle tissues were removed and protein lysates from these tissues were isolated to examine SMN protein levels. The ratio of SMN to actin protein levels was determined by a densitometry analysis. Values represent mean ± SEM. $^{*}P < 0.05$; $^{**}P < 0.01$; $^{***}P < 0.001$.

DISCUSSION

Intraperitoneal administration of the proteasome inhibitor, bortezomib, resulted in a 2-fold increase in SMN protein levels in peripheral tissues of SMA model mice. Affected mice treated with bortezomib alone showed improved righting times but no significant change in lifespan. The lack of a survival benefit in the absence of CNS availability of bortezomib highlights the critical role of SMN in the CNS. Nevertheless, we observed increased myofiber size and number in bortezomib-treated mice and, surprisingly, an increased number of AHCs in the spinal cord. Immunohistochemical examination of the NMJ of bortezomib-treated mice showed increased NMJ size compared with vehicle-treated mice. This improvement in NMJ size could explain the increase in AHC number and the improvement in motor function we observed in treated animals despite the lack of increased SMN levels in the CNS with bortezomib treatment and suggests that treatments that target peripheral tissues may contribute to improving the disease phenotype.

It remains unclear whether SMA is cell autonomous, i.e. caused by the effects of reduced SMN in multiple tissues or solely in motor neurons. In *Drosophila*, a null mutation in Smn is partially rescued by maternal SMN expression that allows development to the larval stage (11). The eventual

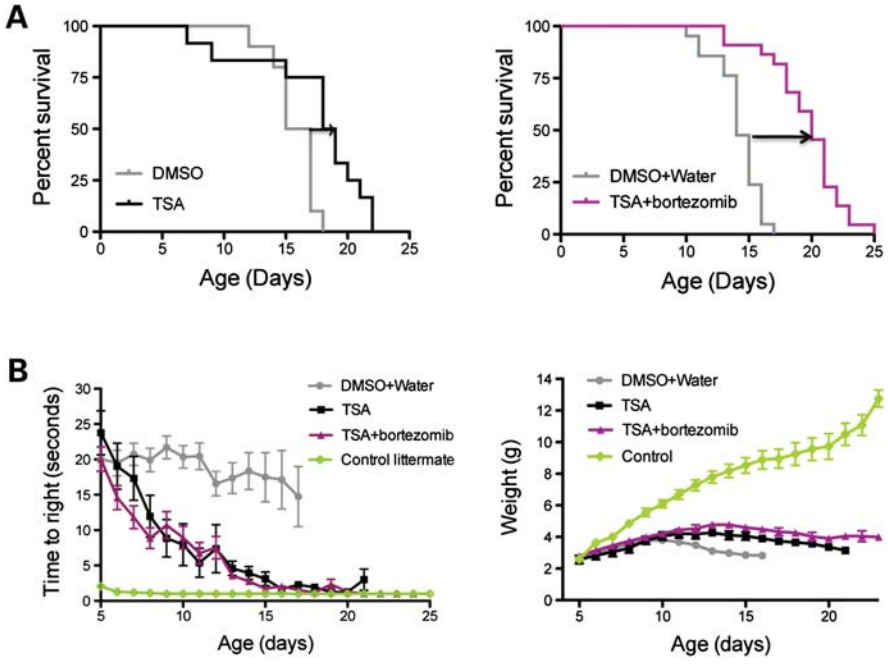

Figure 5. TSA with bortezomib extends survival in SMA mice and improves the SMA phenotype in transgenic mice. SMA mice were treated with daily i.p. injections of TSA (4 mg/kg) and bortezomib (0.075 mg/kg) or vehicle (equal amounts of DMSO and water). A control group was treated with vehicle (DMSO) and TSA alone (4 mg/kg) in the same manner. (**A**) Kaplan–Meier survival curves of SMA mice treated with TSA alone ($n = 12$; median survival = 16 days) or vehicle ($n = 10$; median survival = 18.5 days; log-rank test, $P = 0.007$). (**B**) Survival curves of SMA mice treated with TSA with bortezomib (n = 21; median survival = 20 days) or vehicle (DMSO and water; $n = 21$; median survival = 14 days; log-rank test, $P < 0.0001$). (**C**) Righting times of SMA mice treated with TSA and bortezomib, TSA alone and vehicle. (**D**) Body weights of SMA mice treated with TSA with bortezomib gained more weight than mice treated with either TSA alone ($P < 0.05$) or vehicle ($P < 0.0001$).

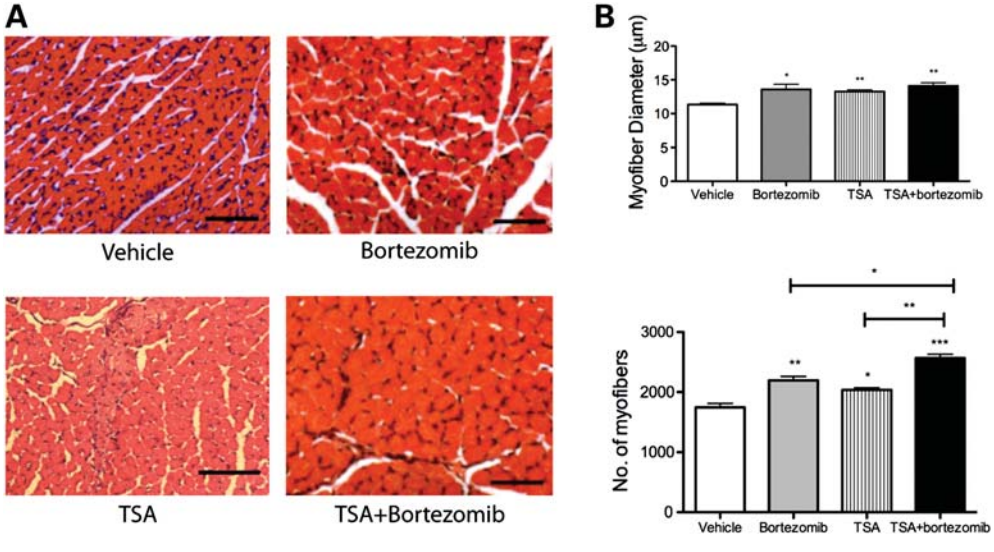

Figure 6. TSA plus bortezomib ameliorates muscle pathology in SMA model mice. SMA mice were treated with vehicle ($n = 3$), bortezomib ($n = 3$), TSA ($n = 3$), TSA + bortezomib ($n = 3$) from P5 to P13. (**A**) Hematoxylin and eosin staining of quadriceps muscles from vehicle- and drug-treated mice. Scale bars: 50 μm. (**B**) Average myofiber diameter was increased with bortezomib treatment ($P < 0.05$), TSA treatment ($P < 0.01$) and TSA + bortezomib ($P < 0.01$). The total TA myofiber number increased with individual bortezomib ($P < 0.01$) and TSA treatments ($P < 0.05$) and increased further with TSA + bortezomib ($P < 0.001$). Values represent mean ± SEM. $^{*}P < 0.05$; $^{**}P < 0.01$; $^{***}P < 0.001$.

depletion of SMN in all tissues results in death and can only be rescued by providing SMN to both muscles and neurons. Depletion of SMN in muscle in flies and mice results in muscle degeneration, indicating that SMN is an essential protein in muscle, as in other tissues (12). Recent work with transgenic mice expressing SMN in muscle under the control of the human skeletal muscle actin promoter showed that SMN restoration in skeletal muscle alone has no appreciable impact on the SMA phenotype (13). However, this does not rule out the possibility that increasing SMN levels in muscle

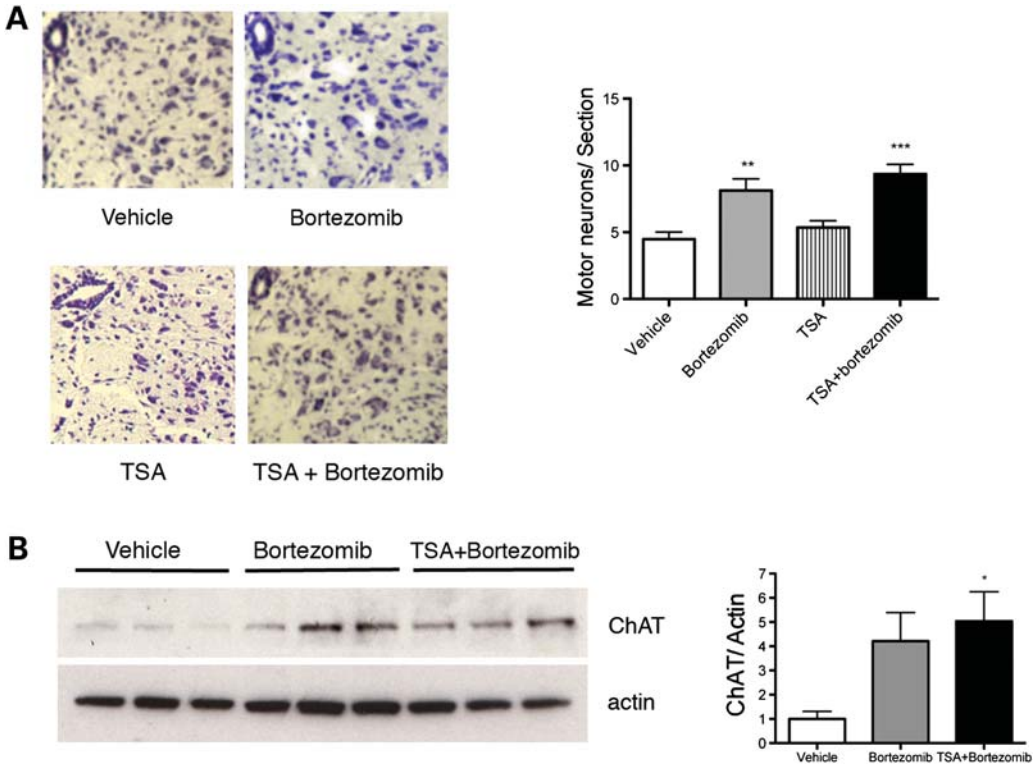

Figure 7. TSA plus bortezomib delays motor neuron death in lumbar spinal cord tissues of SMA model mice. SMA mice treated with vehicle ($n = 3$), bortezomib alone (0.15 mg/kg; $n = 3$), TSA alone (4 mg/kg) or bortezomib (0.075 mg/kg) plus TSA (4 mg/kg; $n = 3$) were sacrificed at P13. (**A**) Nissl-stained sections of ventral spinal cords. Quantitative analysis showed an increase in motor neurons/section in mice treated with bortezomib alone ($P < 0.01$) and a combination of TSA and bortezomib ($P < 0.01$) but not with TSA alone. (**B**) Western blot analysis showed an increase in the ChAT protein levels in spinal cord of bortezomib ($P = 0.056$) and TSA + bortezomib-treated mice compared with vehicle-treated mice ($P < 0.05$). Values represent mean ± SEM. $^{*}P < 0.05$; $^{**}P < 0.01$; $^{***}P < 0.001$.

may enhance whatever beneficial effect repletion of motor neuron SMN may have. Two studies examined inhibitors of the myostatin pathway in SMA mice with contrasting results, one showing a modest extension in lifespan and gross motor function, with delivery of recombinant follistatin, the other detecting no phenotypic improvement in the SMA mice with ActRIIB-Fc treatment or transgenic overexpression of follistatin (14,15). The basis for this discrepancy is unclear; however, the possibility remains that motor neurons may require additional support in peripheral tissues to respond optimally to SMN-based therapeutics. In this study, we found that a 2-fold increase in SMN in peripheral tissues had no effect on the survival of SMA mice, but a similar increase in SMN in animals treated with the CNS penetrant drug, TSA, was sufficient to significantly improve survival. Taken together, these studies would indicate the need for adequate levels of SMN in the CNS for survival.

While this study was ongoing, it was reported that the hydroxamic acid-derived HDAC inhibitor LBH589 markedly increases SMN levels in SMA patient-derived fibroblasts by increasing *SMN2* gene expression and blocking SMN protein degradation (16). We show here that TSA and bortezomib delivered together synergistically increased SMN protein levels in cultured cells and tissues of SMA mice. Mice treated with both drugs lived longer and showed increased body weight. Immunohistochemical analysis of NMJs in mice treated with both drugs showed a cumulative effect on their maturation. Although TSA alone increases SMN protein levels, mitigates muscle and nerve pathophysiology and extends the lifespan of SMA model mice (9), co-administering TSA with bortezomib approximately doubled SMN levels in affected mice compared with TSA alone and further extended survival from 3 to 6 days.

Of particular interest in this study was the finding that bortezomib alone significantly improved the motor function of SMA mice. We observed an increase in SMN protein levels in muscle tissue of treated mice and increases in the number of myofibers and in myofiber diameters. AHC loss was also delayed in bortezomib-treated animals, indicating a central effect of this peripherally acting drug. These SMA mice show motor deficits as early as postnatal day 2, although they do not exhibit significant spinal motor neuron loss at this stage and there is evidence to suggest that defects at the NMJ precede motor neuron loss (17). We found that the NMJs of bortezomib-treated mice were larger than those of vehicle-treated animals. We presume that increased SMN in muscle can positively influence the maturation of the NMJ and survival of motor neurons. It is also possible that inhibition of the proteasome may contribute to muscle improvement by another mechanism independent of SMN. Muscle is a source of neurotrophic factors that are protective of motor neurons (18). Muscle-derived NT-4 is an activity-dependent neurotrophic signal for growth and remodeling of adult motor nerve terminals, and muscle-derived neurotrophic factors are retrogradely transported by motor neurons with

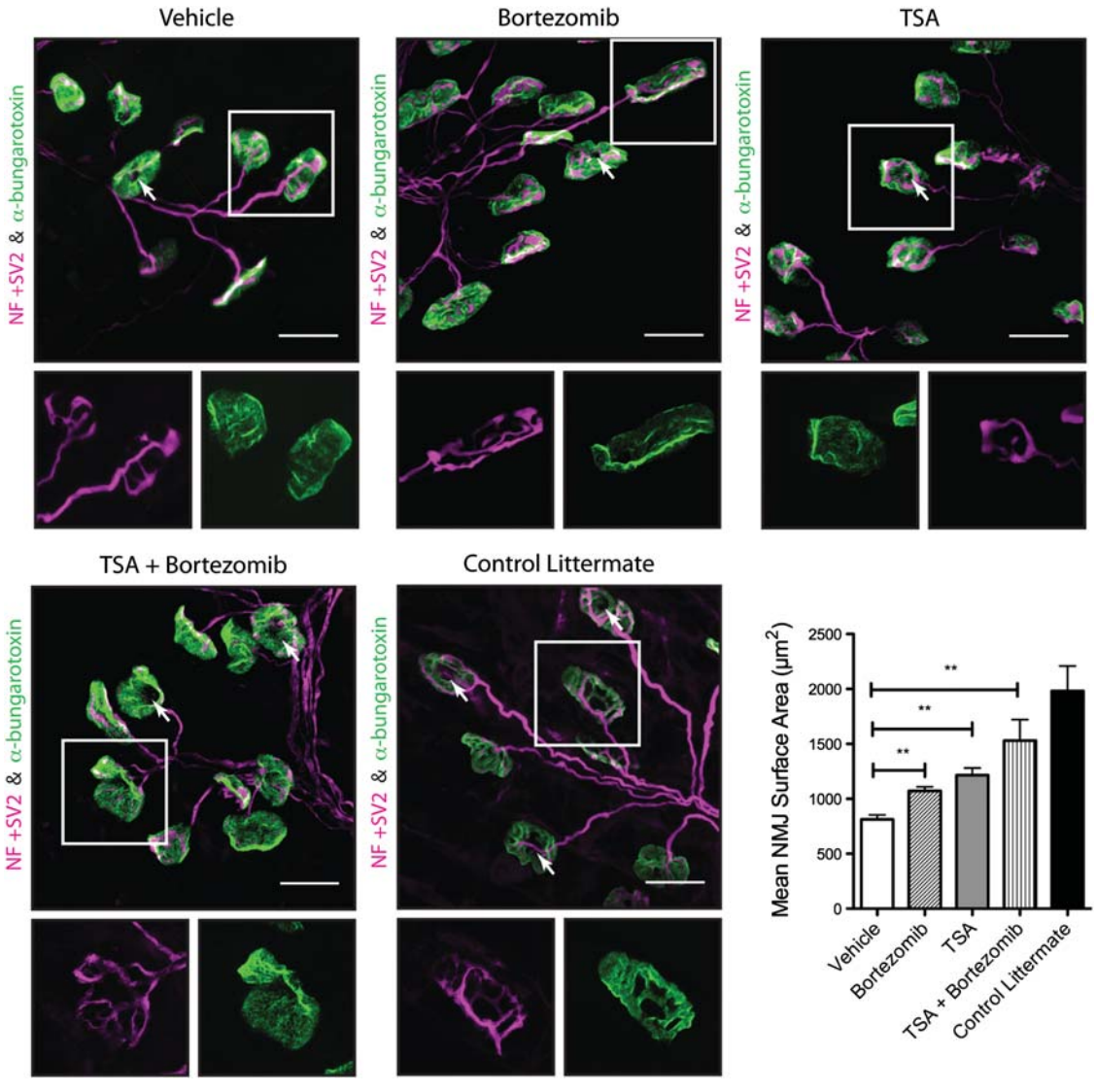

Figure 8. TSA plus bortezomib improves the NMJ. NMJs were isolated from the TA muscles of vehicle- and drug-treated animals at P13. While TSA and bortezomib ($n = 3$) both independently increased NMJ surface area, combining both TSA and bortezomib further improved NMJ size in SMA mice ($P < 0.01$). Values represent mean ± SEM. $^{**}P < 0.01$.

effects at the level of the cell body (19). Recently, muscle-specific insulin-like growth factor 1 expression was shown to reduce spinal cord and muscle pathology in spinal and bulbar muscle atrophy demonstrating that muscle cell signaling can have an effect on motor neuron survival (20). These data indicate that drugs acting peripherally may ameliorate SMA.

The UPS is involved in key events in neuronal development such as neuronal migration and synaptogenesis (21–23), operating at both the pre-synaptic and at the post-synaptic level. Alteration of the ubiquitination of specific substrates due to mutations of ubiquitin conjugating enzymes and ligases may be associated with neurological disease (24–26). Recently, X-linked infantile SMA has been linked to changes in the E1 ubiquitin-activating enzyme (27), suggesting that altered ubiquitination in motor neurons could cause defective development of the motor unit. Maturation of the NMJ involves the pruning of axons from muscle fibers that are innervated by multiple motor neurons, the formation of a highly branched motor axon terminal and the coordinated expansion of the nerve terminal and muscle fiber (28). These events occur during the first 2 weeks of postnatal development in mice with effects on both neuronal development and the growth and maturation of muscle fibers. Interestingly, the proteasome-associated deubiquitinating enzyme Usp14 has been reported to be crucial for the postnatal maturation of the peripheral nervous system by regulating ubiquitin pools at the nerve terminal (29). These and other findings are consistent with a critical role for ubiquitin homeostasis and proteasome activity at the NMJ and could, along with increased SMN levels in peripheral tissues, explain the improvement we observed in the motor unit of SMA mice treated with bortezomib.

Proteasome inhibitors have potential as treatment for a variety of diseases, including immunologic, inflammatory,

metabolic, and neurological disorders, viral diseases, muscular dystrophies and tuberculosis (30,31). Dystrophin and other proteins of the dystrophin glycoprotein complex are degraded by the UPS in the muscle of Duchenne muscular dystrophy patients. Treatment with the proteasome inhibitor MG−132 restores the presence and cellular localization of dystrophin and associated proteins in mdx mice and in skeletal muscle explants from Duchenne muscular dystrophy patients (32,33). Similar results were obtained with bortezomib, a more specific proteasome inhibitor (34). Bortezomib has been approved for clinical use in multiple myeloma and is currently being tested in phase II clinical trials as a possible therapeutic agent for other malignancies (35–38). Two phase I studies involving bortezomib were conducted in children affected by refractory leukemia and solid tumors (39,40). Considerable efforts have been made over the past few years to identify and optimize structurally different proteasome inhibitors using medicinal chemistry or isolating natural compounds with the long-term goal of increasing the beneficial effects and reducing side-effects and toxicity.

Our results provide preclinical support for the UPS as a potential therapeutic target for SMA therapy. Strategies to inhibit SMN degradation can be used in combination with stimulation of SMN gene expression and may enable the use of lower doses of the latter, possibly increasing efficacy and reducing toxicity. Further validation of the role of the UPS in SMA would provide the opportunity to rationally design drugs that target this pathway. Studies elucidating the E3 ligases for SMN and the regulatory events upstream of the proteasome would help to further define the pathway and allow the identification of more specific targets for therapeutic intervention.

MATERIALS AND METHODS

Cell culture and drug treatment

Human fibroblast cell lines from a 3-year-old type I SMA patient (GM03813) and a 2-year-old type I SMA patient (GM09677) were obtained from Coriell Cell Repository. For bortezomib studies, cells were either plated in growth media alone or with bortezomib (Millenium), which was dissolved in water before use. TSA was dissolved in DMSO to a concentration of 50 nM and used to treat cells alone or in combination with bortezomib. The cells were incubated with either bortezomib alone (16 h) or with TSA for 8 h twice, or a combination of TSA and bortezomib overnight. The cells were then harvested for protein isolation and quantification as previously described (5).

Mice and drug treatment

Studies were approved by the National Institute of Neurological Diseases and Stroke Animal Care Committee and performed in accordance with the National Institutes of Health Guide for the Care and Use of Laboratory Animals. Transgenic SMA mice on the FVB background (hSMN2/delta7SMN/mSmn−/−) were purchased from Jackson Laboratories. Animals were genotyped using polymerase chain reaction on tail DNA as previously reported (41).

Bortezomib was dissolved in sterile water to a concentration of 0.15 μg/μl. Pups at postnatal day 5 (P5) were administered 1 μl of bortezomib per gram (for a concentration of 0.15 mg/kg) intraperitoneally using a 33-gauge needle and treated every other day until P13. Control animals received equal volumes of water.

TSA was dissolved in DMSO to a concentration of 4 μg/μl. Pups at P5 were administered 1 μl of TSA per gram daily for a total concentration of 4 mg/kg in a manner similar to bortezomib administration. In order to reduce toxicity with the drug combination, mice were given TSA in the mornings and bortezomib in the evenings.

For one-time measures, pups were weighed and tested for their ability to right themselves. Righting time was defined as the average of two trials of the time required for a pup to turn over after being placed on its back (maximum 30 s). Mice that lost 30% of their body weight and were unable to right themselves were euthanized.

For biochemical studies, the mice were anesthetized with isofluorane and sacrificed by cervical dislocation. Fifty to 100 mg of various tissues (brains, livers, spinal cords, kidneys, limb skeletal muscle) were dissected, flash-frozen in liquid nitrogen and stored at −80°C.

For survival studies, litters were maintained and kept with the mother until P21, after which they were weaned and tested.

Protein extraction and quantification

Tissues were homogenized and incubated in 500 μl of lysis buffer (0.1% NP-40 and 0.5% sodium deoxycholate) for 15 min on ice, and the collected supernatant was sonicated for 10 s before another 15 min incubation. Supernatant was collected after a 15 min centrifuge step at 4°C and stored at −80°C. Protein concentrations were determined by the BCA Protein Assay kit (Pierce) according to the manufacturer's protocol.

Western blotting

Protein lysates (25 μg for wild-type and heterozygous mice, 50–100 μg for SMA mice) were run and separated on a 10% sodium dodecyl sulfate polyacrylamide gel electrophoresis gel and transferred to a polyvinylidene fluoride membrane. These were then probed with a mouse anti-SMN antibody (BD Transduction Laboratories, diluted 1:1000), anti-ChAT antibody (Millipore, dilution 1:1000) and a mouse anti-B-actin antibody (Sigma-Aldrich, diluted 1:10,000).

Pathological analysis

The mice were transcardially perfused with 4% paraformaldehyde. Lumbar spinal cords and distal hind limbs were dissected and post-fixed in the same fixative overnight. Hind limb tissues were decalcified, embedded in paraffin and cross-sectioned at the midpoint of the tibialis anterior muscle. Sections (10 μm) were mounted on slides and stained with hematoxylin and eosin. Digital images were captured using a Zeiss Axiovert 100 M microscope and analyzed with NIH ImageJ software for total TA cross-sectional area

(original magnification, ×5), total tibilias anterior myofiber number (original magnification, ×10) and myofiber diameter (original magnification, ×40). Myofiber diameter was determined by measuring the largest diameter of at least 300 neighboring myofibers per animal. Paraffin-embedded lumbar spinal cord was serially sectioned at 5 μm steps, mounted on slides and stained with Nissl. Images of contiguous sections, 170 μm apart (original magnification, ×10) were analyzed with NIH ImageJ software. The diameter and number of all neurons >25 μm in the region below a line drawn horizontally at the level of the spinal canal were determined.

Neuromuscular junction staining

TA muscles were isolated from P13 or P19 mice and fixed in freshly prepared 2% paraformaldehyde in phosphate buffered saline (PBS) for 4 h on ice. Samples were then transferred to a blocking and permeabilizing solution of 5% normal goat serum and 0.5% Triton X-100 in PBS for 1 h before they were pressed between two glass slides using a binder clip for 15 min, after which the samples were returned to the blocking and permeabilizing solution. The samples were then incubated overnight at 4°C with 1:1000 dilutions of SV2 and 2H3 primary antibodies (Developmental Studies Hybridoma Bank, Iowa City, IA, USA), which target synaptic vesicle protein 2 and neurofilament, respectively. After at least three 1-h washes in PBS with 0.5% Triton X-100, the samples were transferred to blocking and permeabilizing solution with Alexa Fluor 488 goat anti-mouse IgG1 (γ1) (Invitrogen, Carlsbad, CA, USA) and α-bungarotoxin conjugated with Alexa Fluor 594. After incubation overnight at 4°C, samples were washed three times for 1 h and mounted with Vectashield mounting media (Vector Labs, Burlingame, CA, USA) and imaged using an LSM 710 laser scanning microscope (Carl Zeiss, Oberkochen, Germany). NMJ size measurements were determined using the Volocity software (Improvision, Perkin Elmer, Waltham, MA, USA). The objects were found using standard deviation of intensity with a lower limit of two. The objects were then sorted to exclude those with a volume below 300 μm^3 and those touching the edge of the image before they were measured. This staining protocol was adapted from reference (17).

Statistics

Survival and biochemical data were analyzed using the GraphPad Prism software package (version 3; GraphPad Software) and compared statistically with the log-rank test (Kaplan–Meier survival curves), the two-tailed Student's t test or one-way analysis of variance followed by the Newman–Keuls multiple comparison *post hoc* test. Pathological data were analyzed using STATA version 9 software. To compare differences among the three groups, a nonparametric equality of medians test was performed, because the data were not normally distributed. If this was statistically significant, then a pairwise comparison between the two treatment groups was performed using a Mann–Whitney U test. $P \leq 0.05$ was considered significant.

SUPPLEMENTARY MATERIAL

Supplementary Material is available at *HMG* online.

ACKNOWLEDGEMENTS

We thank Vania Cao for her technical assistance in performing animal perfusions and Craig Blackstone for the use of his LSM 710 laser scanning microscope. We would also like to thank Charlotte Sumner for critical reading of this manuscript.

Conflict of Interest statement. None declared.

FUNDING

This work was supported by intramural funds from the National Institute of Neurological Disorders and Stroke (NINDS) at the NIH and a NINDS Competitive Fellowship (to B.G.B.).

REFERENCES

1. Hsieh-Li, H.M., Chang, J.G., Jong, Y.J., Wu, M.H., Wang, N.M., Tsai, C.H. and Li, H. (2000) A mouse model for spinal muscular atrophy. *Nat. Genet.*, **24**, 66–70.
2. Lefebvre, S., Burglen, L., Reboullet, S., Clermont, O., Burlet, P., Viollet, L., Benichou, B., Cruaud, C., Millasseau, P., Zeviani, M. *et al.* (1995) Identification and characterization of a spinal muscular atrophy-determining gene. *Cell*, **80**, 155–165.
3. McAndrew, P.E., Parsons, D.W., Simard, L.R., Rochette, C., Ray, P.N., Mendell, J.R., Prior, T.W. and Burghes, A.H. (1997) Identification of proximal spinal muscular atrophy carriers and patients by analysis of SMNT and SMNC gene copy number. *Am. J. Hum. Genet.*, **60**, 1411–1422.
4. Prior, T.W., Swoboda, K.J., Scott, H.D. and Hejmanowski, A.Q. (2004) Homozygous SMN1 deletions in unaffected family members and modification of the phenotype by SMN2. *Am. J. Med. Genet. A*, **130**, 307–310.
5. Burnett, B.G., Munoz, E., Tandon, A., Kwon, D.Y., Sumner, C.J. and Fischbeck, K.H. (2009) Regulation of SMN Protein Stability. *Mol. Cell. Biol.*, **29**, 1107–1115.
6. Chang, H.C., Hung, W.C., Chuang, Y.J. and Jong, Y.J. (2004) Degradation of survival motor neuron (SMN) protein is mediated via the ubiquitin/proteasome pathway. *Neurochem. Int.*, **45**, 1107–1112.
7. Kisselev, A.F., Callard, A. and Goldberg, A.L. (2006) Importance of the different proteolytic sites of the proteasome and the efficacy of inhibitors varies with the protein substrate. *J. Biol. Chem.*, **281**, 8582–8590.
8. Adams, J., Palombella, V.J., Sausville, E.A., Johnson, J., Destree, A., Lazarus, D.D., Maas, J., Pien, C.S., Prakash, S. and Elliott, P.J. (1999) Proteasome inhibitors: a novel class of potent and effective antitumor agents. *Cancer Res.*, **59**, 2615–2622.
9. Avila, A.M., Burnett, B.G., Taye, A.A., Gabanella, F., Knight, M.A., Hartenstein, P., Cizman, Z., Di Prospero, N.A., Pellizzoni, L., Fischbeck, K.H. *et al.* (2007) Trichostatin A increases SMN expression and survival in a mouse model of spinal muscular atrophy. *J. Clin. Invest.*, **117**, 659–671.
10. Narver, H.L., Kong, L., Burnett, B.G., Choe, D.W., Bosch-Marce, M., Taye, A.A., Eckhaus, M.A. and Sumner, C.J. (2008) Sustained improvement of spinal muscular atrophy mice treated with trichostatin A plus nutrition. *Ann. Neurol.*, **64**, 465–470.
11. Chan, Y.B., Miguel-Aliaga, I., Franks, C., Thomas, N., Trulzsch, B., Sattelle, D.B., Davies, K.E. and van den Heuvel, M. (2003) Neuromuscular defects in a Drosophila survival motor neuron gene mutant. *Hum. Mol. Genet.*, **12**, 1367–1376.
12. Cifuentes-Diaz, C., Frugier, T., Tiziano, F.D., Lacene, E., Roblot, N., Joshi, V., Moreau, M.H. and Melki, J. (2001) Deletion of murine SMN exon 7 directed to skeletal muscle leads to severe muscular dystrophy. *J. Cell Biol.*, **152**, 1107–1114.

13. Gavrilina, T.O., McGovern, V.L., Workman, E., Crawford, T.O., Gogliotti, R.G., DiDonato, C.J., Monani, U.R., Morris, G.E. and Burghes, A.H. (2008) Neuronal SMN expression corrects spinal muscular atrophy in severe SMA mice while muscle-specific SMN expression has no phenotypic effect. *Hum. Mol. Genet.*, **17**, 1063–1075.
14. Rose, F.F. Jr, Mattis, V.B., Rindt, H. and Lorson, C.L. (2009) Delivery of recombinant follistatin lessens disease severity in a mouse model of spinal muscular atrophy. *Hum. Mol. Genet.*, **18**, 997–1005.
15. Sumner, C.J., Wee, C.D., Warsing, L.C., Choe, D.W., Ng, A.S., Lutz, C. and Wagner, K.R. (2009) Inhibition of myostatin does not ameliorate disease features of severe spinal muscular atrophy mice. *Hum. Mol. Genet.*, **18**, 3145–3152.
16. Garbes, L., Riessland, M., Holker, I., Heller, R., Hauke, J., Trankle, C., Coras, R., Blumcke, I., Hahnen, E. and Wirth, B. (2009) LBH589 induces up to 10-fold SMN protein levels by several independent mechanisms and is effective even in cells from SMA patients non-responsive to valproate. *Hum. Mol. Genet.*, **18**, 3645–3658.
17. Le, T.T., Pham, L.T., Butchbach, M.E., Zhang, H.L., Monani, U.R., Coovert, D.D., Gavrilina, T.O., Xing, L., Bassell, G.J. and Burghes, A.H. (2005) SMNDelta7, the major product of the centromeric survival motor neuron (SMN2) gene, extends survival in mice with spinal muscular atrophy and associates with full-length SMN. *Hum. Mol. Genet.*, **14**, 845–857.
18. Griesbeck, O., Parsadanian, A.S., Sendtner, M. and Thoenen, H. (1995) Expression of neurotrophins in skeletal muscle: quantitative comparison and significance for motoneuron survival and maintenance of function. *J. Neurosci. Res.*, **42**, 21–33.
19. DiStefano, P.S., Friedman, B., Radziejewski, C., Alexander, C., Boland, P., Schick, C.M., Lindsay, R.M. and Wiegand, S.J. (1992) The neurotrophins BDNF, NT-3, and NGF display distinct patterns of retrograde axonal transport in peripheral and central neurons. *Neuron*, **8**, 983–993.
20. Palazzolo, I., Stack, C., Kong, L., Musaro, A., Adachi, H., Katsuno, M., Sobue, G., Taylor, J.P., Sumner, C.J., Fischbeck, K.H. *et al.* (2009) Overexpression of IGF-1 in muscle attenuates disease in a mouse model of spinal and bulbar muscular atrophy. *Neuron*, **63**, 316–328.
21. Muralidhar, M.G. and Thomas, J.B. (1993) The Drosophila bendless gene encodes a neural protein related to ubiquitin-conjugating enzymes. *Neuron*, **11**, 253–266.
22. Hegde, A.N. and Upadhya, S.C. (2007) The ubiquitin-proteasome pathway in health and disease of the nervous system. *Trends Neurosci.*, **30**, 587–595.
23. Yi, J.J. and Ehlers, M.D. (2007) Emerging roles for ubiquitin and protein degradation in neuronal function. *Pharmacol. Rev.*, **59**, 14–39.
24. Liu, Y., Fallon, L., Lashuel, H.A., Liu, Z. and Lansbury, P.T. Jr (2002) The UCH-L1 gene encodes two opposing enzymatic activities that affect alpha-synuclein degradation and Parkinson's disease susceptibility. *Cell*, **111**, 209–218.
25. Nawaz, Z., Lonard, D.M., Smith, C.L., Lev-Lehman, E., Tsai, S.Y., Tsai, M.J. and O'Malley, B.W. (1999) The Angelman syndrome-associated protein, E6-AP, is a coactivator for the nuclear hormone receptor superfamily. *Mol. Cell. Biol.*, **19**, 1182–1189.
26. Trockenbacher, A., Suckow, V., Foerster, J., Winter, J., Krauss, S., Ropers, H.H., Schneider, R. and Schweiger, S. (2001) MID1, mutated in Opitz syndrome, encodes an ubiquitin ligase that targets phosphatase 2A for degradation. *Nat. Genet.*, **29**, 287–294.
27. Ramser, J., Ahearn, M.E., Lenski, C., Yariz, K.O., Hellebrand, H., von Rhein, M., Clark, R.D., Schmutzler, R.K., Lichtner, P., Hoffman, E.P. *et al.* (2008) Rare missense and synonymous variants in UBE1 are associated with X-linked infantile spinal muscular atrophy. *Am. J. Hum. Genet.*, **82**, 188–193.
28. Sanes, J.R. and Lichtman, J.W. (1999) Development of the vertebrate neuromuscular junction. *Annu. Rev. Neurosci.*, **22**, 389–442.
29. Chen, P.C., Qin, L.N., Li, X.M., Walters, B.J., Wilson, J.A., Mei, L. and Wilson, S.M. (2009) The proteasome-associated deubiquitinating enzyme Usp14 is essential for the maintenance of synaptic ubiquitin levels and the development of neuromuscular junctions. *J. Neurosci.*, **29**, 10909–10919.
30. Jung, T., Catalgol, B. and Grune, T. (2009) The proteasomal system. *Mol. Aspects Med.*, **30**, 191–296.
31. Meiners, S., Ludwig, A., Stangl, V. and Stangl, K. (2008) Proteasome inhibitors: poisons and remedies. *Med. Res. Rev.*, **28**, 309–327.
32. Bonuccelli, G., Sotgia, F., Schubert, W., Park, D.S., Frank, P.G., Woodman, S.E., Insabato, L., Cammer, M., Minetti, C. and Lisanti, M.P. (2003) Proteasome inhibitor (MG-132) treatment of mdx mice rescues the expression and membrane localization of dystrophin and dystrophin-associated proteins. *Am. J. Pathol.*, **163**, 1663–1675.
33. Assereto, S., Stringara, S., Sotgia, F., Bonuccelli, G., Broccolini, A., Pedemonte, M., Traverso, M., Biancheri, R., Zara, F., Bruno, C. *et al.* (2006) Pharmacological rescue of the dystrophin-glycoprotein complex in Duchenne and Becker skeletal muscle explants by proteasome inhibitor treatment. *Am. J. Physiol. Cell Physiol.*, **290**, C577–C582.
34. Bonuccelli, G., Sotgia, F., Capozza, F., Gazzerro, E., Minetti, C. and Lisanti, M.P. (2007) Localized treatment with a novel FDA-approved proteasome inhibitor blocks the degradation of dystrophin and dystrophin-associated proteins in mdx mice. *Cell Cycle*, **6**, 1242–1248.
35. Armand, J.P., Burnett, A.K., Drach, J., Harousseau, J.L., Lowenberg, B. and San Miguel, J. (2007) The emerging role of targeted therapy for hematologic malignancies: update on bortezomib and tipifarnib. *Oncologist*, **12**, 281–290.
36. Davis, N.B., Taber, D.A., Ansari, R.H., Ryan, C.W., George, C., Vokes, E.E., Vogelzang, N.J. and Stadler, W.M. (2004) Phase II trial of PS-341 in patients with renal cell cancer: a University of Chicago phase II consortium study. *J. Clin. Oncol.*, **22**, 115–119.
37. Faderl, S., Rai, K., Gribben, J., Byrd, J.C., Flinn, I.W., O'Brien, S., Sheng, S., Esseltine, D.L. and Keating, M.J. (2006) Phase II study of single-agent bortezomib for the treatment of patients with fludarabine-refractory B-cell chronic lymphocytic leukemia. *Cancer*, **107**, 916–924.
38. Nencioni, A., Grunebach, F., Patrone, F., Ballestrero, A. and Brossart, P. (2007) Proteasome inhibitors: antitumor effects and beyond. *Leukemia*, **21**, 30–36.
39. Blaney, S.M., Bernstein, M., Neville, K., Ginsberg, J., Kitchen, B., Horton, T., Berg, S.L., Krailo, M. and Adamson, P.C. (2004) Phase I study of the proteasome inhibitor bortezomib in pediatric patients with refractory solid tumors: a Children's Oncology Group study (ADVL0015). *J. Clin. Oncol.*, **22**, 4804–4809.
40. Horton, T.M., Pati, D., Plon, S.E., Thompson, P.A., Bomgaars, L.R., Adamson, P.C., Ingle, A.M., Wright, J., Brockman, A.H., Paton, M. *et al.* (2007) A phase 1 study of the proteasome inhibitor bortezomib in pediatric patients with refractory leukemia: a Children's Oncology Group study. *Clin. Cancer Res.*, **13**, 1516–1522.
41. Kernochan, L.E., Russo, M.L., Woodling, N.S., Huynh, T.N., Avila, A.M., Fischbeck, K.H. and Sumner, C.J. (2005) The role of histone acetylation in SMN gene expression. *Hum. Mol. Genet.*, **14**, 1171–1182.